Plant Design for Deterministic Control of STEMs and Tape-Springs

by

Ross L. Hatton

Submitted to the Department of Mechanical Engineering
in partial fulfillment of the requirements for the degree of

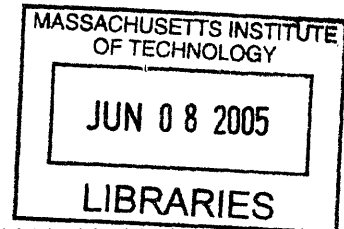Bachelor of Science in Mechanical Engineering

at the

MASSACHUSETTS INSTITUTE OF TECHNOLOGY

May 2005   [June 2005]

Author ....

Department of Mechanical Engineering
May 6, 2005

Certified by...

Alexander H. Slocum
Professor of Mechanical Engineering
Thesis Supervisor

Accepted by ....

Ernest G. Cravalho
Undergraduate Officer

Plant Design for Deterministic Control of STEMs and Tape-Springs

by

Ross L. Hatton

Submitted to the Department of Mechanical Engineering
on May 6, 2005, in partial fulfillment of the
requirements for the degree of
Bachelor of Science in Mechanical Engineering

Abstract

In this thesis, the limits of conventional linear actuators for long stroke applications are discussed, and tape-spring based actuators such as the STEM are introduced as an alternative solution. While the literature contains several assessments of self-deploying tape-springs, little exists in the area of closed loop deterministic control of such mechanisms. This thesis adapts the existing models of tape springs to form a framework for the study of closed loop controllable tape springs. Included is an evaluation of the validity of the prevailing first order model for a coiled tape-spring. Lastly, several avenues for future research are suggested.

Thesis Supervisor: Alexander H. Slocum
Title: Professor of Mechanical Engineering

Acknowledgments

Contents

List of Figures

Chapter 1

Introduction

Linear actuators are generally limited in their effective strain (maximum over minimum device length, including packaging) by geometric concerns. Either their driving impetus is limited in its range of motion, as in a piston linkage or Watt coupling, or there is a limit to the space available for retraction of the mechanism when the desired position is close to the body of the actuator, as with a linear motor or a rack and pinion setup. Telescoping mitigates this geometric problem to some extent, as is also the case with push chain configurations, but at the cost of increased complexity and part count. Tape-spring drives (such as the STEM, or Split Tube Extendable Member), a class of actuators well known in the field of deployable structures for space applications [10], but of uneven notoriety elsewhere, replace the numerous parts of a telescoping device with locking flexures, countering many of the drawbacks of collapsible actuators.

This thesis will examine the supporting mechanisms necessary to make a deterministic and hysteresis-free rotary-to-linear transmission element from tape-springs in general and specifically STEMs. It will further consider the dynamics of an actuator built with the described transmission and determine when the traditional first order model for extending tape-springs fails and must be replaced by a more complete model.

1.1 Traditional linear actuators

Most commonly found electric linear actuators involve a local rotational input and some form of transmission system. Chief exceptions to this rule are linear electromechanical motors; these can however be grouped with rack and pinion devices for the current geometric examination. The simplest transmissions for any of these devices is a "friction drive" which maintains rolling contact between a moving bar and a powered wheel, matching the motion of the bar to that of the wheel and extending any excess length of bar behind the actuator case. Telescoping devices use cabling to drive multiple bars that nest or stack at lesser extensions. Similar in concept to the telescoping devices are scissor linkages, which unfold from a packed configuration to extend.

Rack and pinion mechanisms (such as that pictured in Figure 1-1(a)), along with devices making use of pinch wheels to maintain rolling contact through friction (friction drives), benefit greatly from their simplicity. The moving bar is a single part and can be constrained with a single bearing at the base to minimize lateral deflection. As long as the gear teeth remain engaged or slip is prevented, the position of the bar can be measured from the wheel axle. The equivalent moment of inertia of the bar to the motor axis remains constant through the travel of the device, allowing for travels as great as surrounding space and the bearings used will allow. The need for surrounding space, specifically directly behind the actuator housing, prevents the use of these actuators in many long stroke applications. They are, however, still used extensively where space is available, such as retractable security gates. Through reciprocity, rolling contact drives are, of course, used everywhere as the common wheel.

Where lack of room behind an actuator prevents use of a rack and pinion, various telescoping mechanisms come into play. The key defining feature of any telescoping mechanism is that it is made up of sliding pieces offset from each other in a direction normal to the axis of extension. Common forms include traditional telescopes with tubes nested in each other, where the offset is radial, and sets of parallel bars not nested in each other, like the lift in Figure 1-1(b). While the use of multiple members

gives telescoping devices versatility, it also impacts their robustness. The bearing on each link makes the whole system more compliant, and increased bearing quality and cost can only compensate to a certain extent. Telescopes typically have longer package lengths than other linear actuators, the elements not being able to pack into a length smaller than their own. Decreasing the individual link length adds to the number of error-producing bearings and thus has its own limits.

Folding drives such as scissor linkages (Figure 1-1(c)) rotate their links for storage, and such devices are able to avoid the minimum length requirements of the telescope. The scissor has its own weaknesses, however. At low extensions, the force required to move the linkage by squeezing the base is very great, increasing the size of the motor needed or requiring that the linkage not be allowed to retract beyond a certain limit. Scissors also have the weakness that they are prone to lateral instability unless two are used side by side with common axles.

1.2   Rollup actuators

Research in the area of compact deployable structures has largely been driven by the aerospace sector, where the small launch volumes of spacebound cargoes necessitate that antennas and instrument booms extend once the satellite has reached orbit. Theatre and its technical support is an area which has made use of aerospace advances in extensions. Special effects on stage often require an actor to ascend to or descend from the ceiling. Dressing the set requires that workers be able to reach the lighting racks, often in places where catwalks are impractical installations.

Two key extension mechanisms in use in these and other areas are the push chain and various tape-spring drives, notably the STEM. These actuators have in common a retraction mechanism involving a change in configuration which alters stiffness, allowing the column to be wound on a reel.

Push chains are generally chains with one direction of flexure. As they are deployed, they pass through a mechanism that arranges the links into a column capable of supporting a compressive load as shown in Figure 1-2(a). Retracting the chain
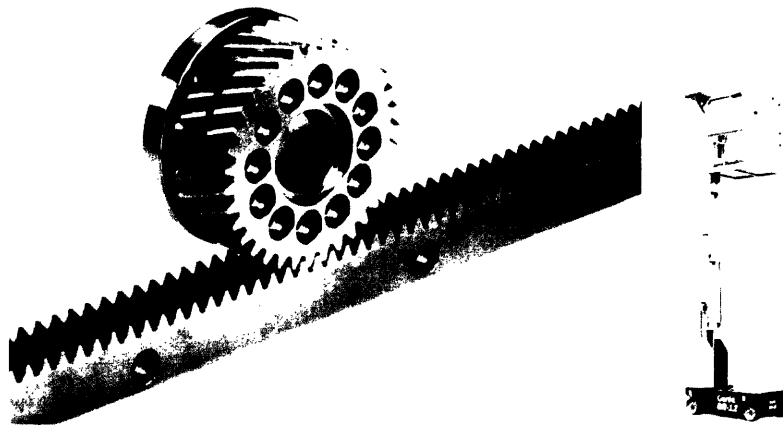
(a) Rack and pinion [1]

(b) Tele-scoping lift [4]
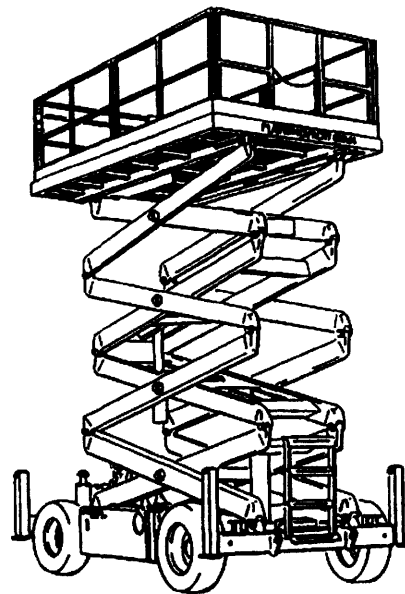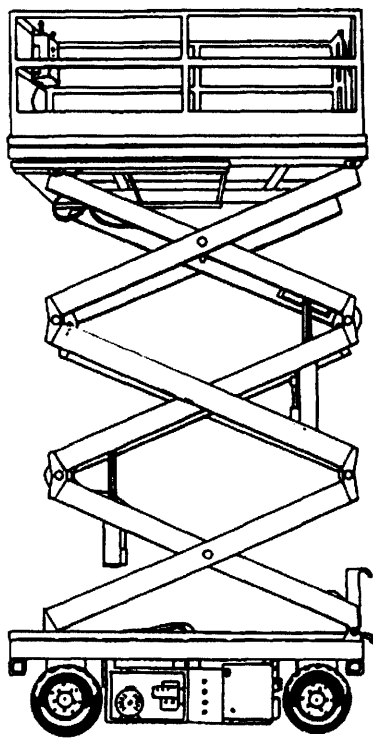
SCISSOR LIFT AERIAL WORK PLATFORM

(c) Scissor lift [3]

Figure 1-1: Traditional linear actuators

pulls it back through the configuration mechanism, which reverses the arrangement, allowing the chain to bend again for rolling purposes. In single chain configurations, the links have a single axle connecting them when in the flexible state and a pin parallel to the axle in the stiff configuration. Multiple chain models exist as well, with the two coils of links sending out chains through a zipper-like mechanism. Two kinds of links are used, one with a foldout hook in the middle and one with a catch for the hook, with the links either alternating on each chain or each chain being homogenous. The chief weaknesses of push chain actuators are the number and precision of parts required and the guidance needed on the load so as not to fall out of the rigid configuration.

Tape-spring actuators maintain the storage benefits of push chains while replacing the many necessary joints with a continuous flexure. Most commonly encountered in steel measuring tapes, tape-springs are strips of elastic material with transverse curvature in their cross section. For small bending deflections, the strips act as cantilevers. Beyond a certain point, however, the tape locally snaps into a flat strip. In the flat form, the spring bends with constant radius, owing to the residual stresses from the shape change. Once this bend is present, it can be moved or extended with much less force than was initially required to achieve it. This property allows the tape to be moved easily between its rigid straight form and a reserve magazine of flattened tape wound on a drum.

While measuring tapes can take some amount of axial or lateral load before buckling, especially at short extensions, their open-section nature leaves them prone to twisting. The tape is already prone to twisting when bent towards its concave surface, a phenomena which contributes to the much lower bending strength and force required to achieve snap-through when the forces are towards the concave surface. Additional twisting magnifies this weakness. Several approaches are used in practice to close the section and reinforce the tape against both external torques and its own inclinations to twist, increasing the length to which the straightened part can be extended and the load which can be moved. Aerospace applications make extensive use of the STEM, a tape spring which curls into a full tube as it extends. At least one
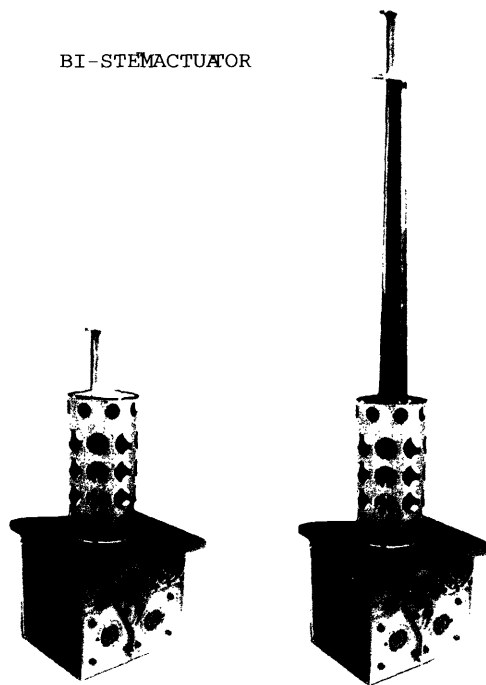
Guided structure

Attachment link
Driving rollers
Vertical guides
Curved guide
Fixations
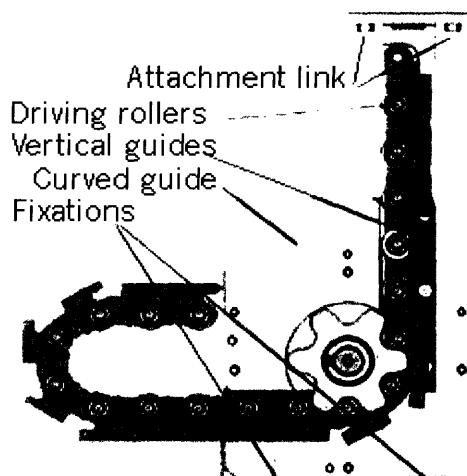
(a) Push chain [6]

BI-STEMACTUATOR

(b) RibbonLift™[5]

(c) STEM (Storable Tubular Extendable Member) [13]

Figure 1-2: Rollup actuators

supplier of theatrical equipment offers a lift that incorporates three tape-springs that zip together at the edges, forming a triangular column.

Triangularly interlaced tapes, sold commercially as RibbonLifts™ by the company of that name [5], gain strength both through the stabilizing effects of the edge constraints and through the increased moment of inertia the column gains from the space included in the triangle. The STEM is a single tape-spring, but where the common carpenter's tape subtends an arc of $50° - 70°$, the STEM curls into a full circle and often overlaps itself, with an arc of $360° - 430°$ [10]. The STEM is thus also a closed section with a substantial enclosed area, but without the edge on edge contact points of the zippered mechanism and with a packaging mechanism that requires less of a footprint in the plane normal to the axis of extension.

1.3   Deterministic plant model

The literature surrounding tape springs is primarily concerned with the solid mechanics which model their behavior, with little concern for their implementation as linear actuators for feedback control. When dynamics are considered, it is generally with respect to the free extension of STEMs as antennas or the use of open tape-springs as locking hinges for panels such as solar panels. It is the purpose of this thesis to examine the necessary features to use the STEM as a repeatable deterministic transmission element in the plant of a feedback system.

Key to using the STEM to drive a load in response to a signal is the maintenance of tension at the point where the tape-spring leaves the storage drum. Descriptions of the unrolling process of the STEM read at first glance as if it unwraps smoothly from the reel under impetus from the energy stored in it during wrapping and that all that is needed to control the end position is a motor to counter or augment the spring force as necessary, and a guide to ensure that it leaves the spool in the right direction. This view ignores the tendency of the tape to pull away from the spool if the straightened section is pushed. Loss of tight wrapping behavior hurts any feedback control attempted on the system as it partially decouples the position of the drum
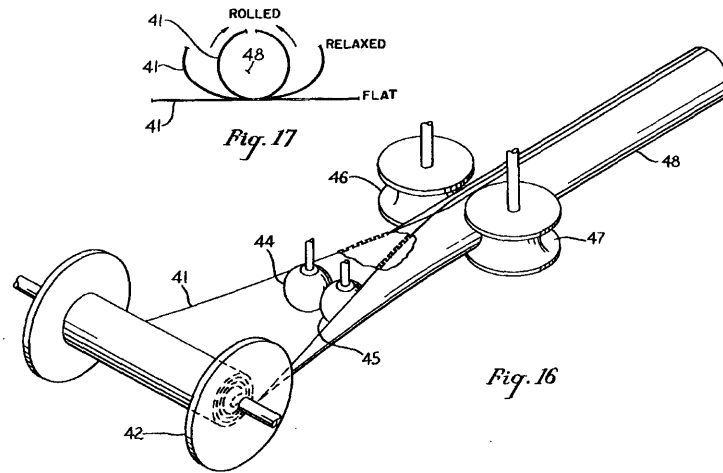
(a) STEM and support mechanism
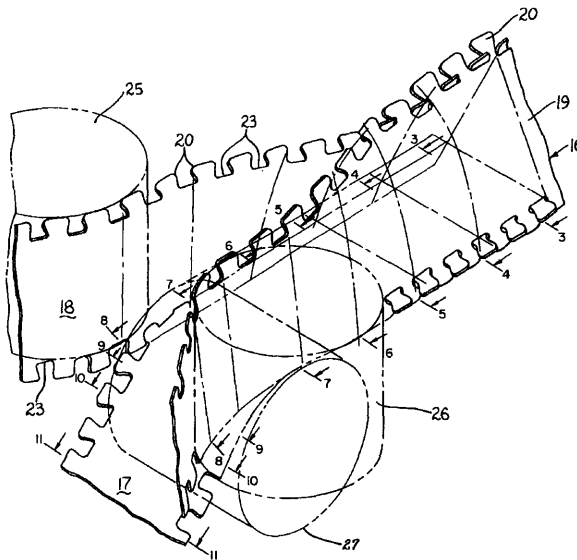
(b) Triangular tape zipping method

Figure 1-3: Patent drawings of tape-spring actuators [2]

from the tip, disturbing the transfer function for the plant.

A configuration which gets around the above limitation is to drive the STEM at the point where it forms a full tube, directly coupling the movement of the rigid member to that of the controlled motor. The importance of tight wrapping becomes an issue of maintaining a deterministic inertia for the system, which can be achieved by putting a small opposing torque (backtorque) on the takeup reel, ensuring that the torque is sufficient to overcome the natural unwinding torque of the tape-spring and accelerate the drum and any spring wrapped around it to match the drive acceleration while maintaining enough tension at the wrapping point to prevent any wrapping irregularities. A schematic for the described system is shown in Figure 2-1, and forms the basis for the modeling in future chapters.

Chapter 2

Physical Model

A first order model for the implementation described in Chapter 1 can be arrived at through Rimrott's examinations of the STEM as a machine element [9][10]. Appropriate use of his results, combined with fresh analysis where the current configuration differs from that envisioned by Rimrott, provides a model for the system which is accurate for all but the longest tape springs. As Rimrott notes in passing [9], he disregards the effect of the changes in wrap diameter at different extensions in the interest of maintaining manageable equations. Given the advances in computation power in the forty years since his paper was published and this work's emphasis on precision control, a reëvaluation of the effect of varying diameter seems prudent and will appear in Chapter 3.

As a frame of reference, the convention used will be that the tip of an entirely coiled tape is at $x = 0$ and that of a fully extended tape is at $x = l$.

2.1   Inertia of the system

The moment of inertia of the system as seen at the drive axis of the pinch bearing, J_J, is a combination of the inertia of the tape, J_T and that of the various rotors in the mechanism, J_R as seen from the same point:
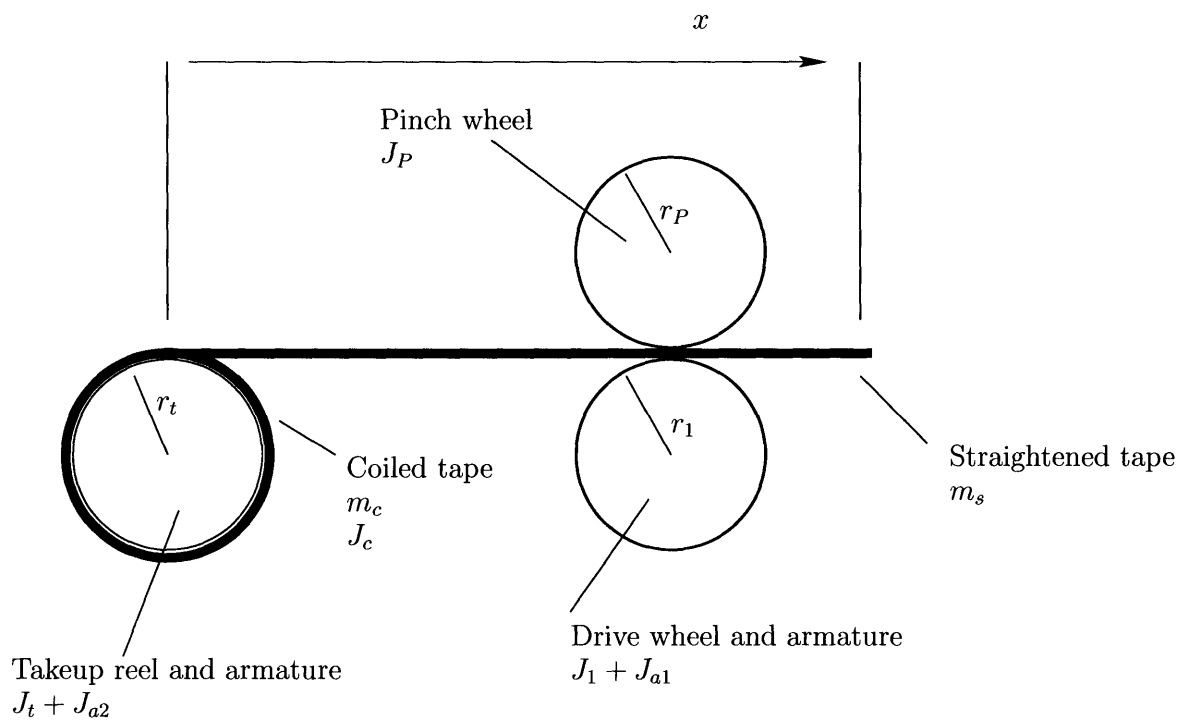
$$J_J = J_T + J_R.$$ (2.1)

17

Figure 2-1: Schematic of proposed system

Table 2.1: Table of symbols

Symbol	Units	Name	Figure
a_{max}	$m \cdot s^{-2}$	Maximum desired acceleration	
α	rad	Half-overlap angle of curled STEM	2-3
d_0	m	STEM tube diameter	2-3
E	Pa	Young's modulus of tape	
F_c	N	Force on tape from unwinding coil	
J_1	$kg \cdot m^2$	Inertia of driving pinch wheel	2-1
J_{a1}	$kg \cdot m^2$	Inertia of driving motor's armature	2-1
J_{a2}	$kg \cdot m^2$	Inertia of backtorque motor's armature	2-1
J_α	$kg \cdot m^2$	Inertia of pinch wheels and straightened tape	2-2
J_β	$kg \cdot m^2$	Inertia of coil and takeup apparatus	2-2
$J_\beta^\star$	$kg \cdot m^2$	Inertia of coil and takeup apparatus in full model	3-1
J_J	$kg \cdot m^2$	Total inertia of the system, as seen at the driving motor	
$J_J^\star$	$kg \cdot m^2$	Total inertia of the system in full model	
J_c	$kg \cdot m^2$	Inertia of tape coiled on reel	2-1
$J_c^\star$	$kg \cdot m^2$	Inertia of tape coiled on reel in full model	3-1
J_P	$kg \cdot m^2$	Inertia of idle pinch wheel	2-1
J_R	$kg \cdot m^2$	Total inertia of all rotors and armatures	
J_T	$kg \cdot m^2$	Total effective inertia of tape-spring	
J_t	$kg \cdot m^2$	Inertia of takeup reel	2-1
l	m	Length of tape-spring	
M_M	kg	Total mass equivalent of the system's moving parts	
M_T	kg	Total mass equivalent of the tape in the system	
m_s	kg	Mass of the tape off reel	2-1
m_c	kg	Mass of the tape wrapped on the reel	2-1
ν		Poisson's ratio of the tape	
ϕ	rad	Curl of straightened STEM	2-3
r_1	m	Radius of drive wheel	2-1
r_o	m	Outer radius of coil in detailed model	
r_P	m	Radius of idle pinch roller	2-1
r_t	m	Radius of takeup reel	2-1
T	N	Tension in tape between reel and drive	2-4
t	m	Thickness of tape	2-3
τ_1	$N \cdot m$	Driving torque of actuator	2-4
$\bar{\tau}_1$	$N \cdot m$	DC offset countering backtorque	
$\tilde{\tau}_1$	$N \cdot m$	Torque for position control	
τ_2	$N \cdot m$	Backtorque on takeup reel	2-4
τ_c	$N \cdot m$	Coil unwinding torque as seen at driving axis	
$\tau_c^\star$	$N \cdot m$	Coil unwinding torque in full model as seen at driving axis	
τ_{ct}	$N \cdot m$	Coil unwinding torque, as seen at coil's axis	2-4
$\tau_{ct}^\star$	$N \cdot m$	Coil unwinding torque, as seen at coil's axis	2-4
V_c	J	Energy stored in coil	
x	m	distance from coil to tip of extended section.	2-1

2.1.1 Tape-spring

The inertia of a tape-spring with density per unit length ρ and length l can be considered by dividing the tape into two parts, the straightened part with mass $m_s(x) = \rho x$ and the coiled part with mass $m_c(x) = \rho(l - x)$ and moment of inertia $J_c(x)$. As seen by the driving motor, the total effective moment of inertia of the tape, J_T, is

$$J_T = m_s(x)r_1^2 + J_c\frac{r_1^2}{r_t^2}. \tag{2.2}$$

As we are for now considering the wrapping distance to be constant, we can make the substitution

$$J_c(x) = m_c(x)r_t^2. \tag{2.3}$$

Further, as the total mass of the tape, M_T, is

$$M_T = m_s(x) + m_c(x), \tag{2.4}$$

The effective moment of inertia of the tape can be seen to be

$$J_T = M_T r_1^2. \tag{2.5}$$

2.1.2 Rotors

Several hubs and rotors add inertia beyond that of the tape. These elements are the two motor armatures, J_{a1} and J_{a2}, the drive wheel, J_1, the idle pinch wheel, J_P and the takeup reel, J_t, which shares diameter r_t with the coil under our current model. Allowing for design decisions possibly requiring different radii on the individual rotors, the effective inertia at the drive axis for the rotors, J_R is

$$J_R = J_{a1} + J_1 + J_P \left(\frac{r_1}{r_P}\right)^2 + (J_{a2} + J_t)\left(\frac{r_1}{r_t}\right)^2. \tag{2.6}$$

If the rotor selection can be made to set $r_1 = r_P = r_t$, the rotor inertia simplifies to

$$J_{R_s} = J_{a1} + J_1 + J_P + J_{a2} + J_t. \tag{2.7}$$

2.1.3 Summation of inertias

Substituting Equations (2.5) and (2.6) into Equation (2.1), J_J is seen to be

$$J_J = M_T r_1^2 + J_{a1} + J_1 + J_P \left(\frac{r_1}{r_P}\right)^2 + (J_{a2} + J_t) \left(\frac{r_1}{r_t}\right)^2. \tag{2.8}$$

The equivalent linear mass of the system, M_M is thus

$$M_M = M_T + \frac{J_{a1} + J_1}{r_1^2} + \frac{J_P}{r_P^2} + \frac{J_{a2} + J_t}{r_t^2}. \tag{2.9}$$

A different grouping of inertias that will prove useful later is to refer to the straightened section and the pinch bearing as J_α and to the coil and its associated rotors as J_β, as grouped in Figure 2-2:

$$J_\alpha = m_s(x)r_1^2 + J_{a1} + J_1 + J_P \left(\frac{r_1}{r_P}\right)^2 \tag{2.10}$$

$$J_\beta = (J_c(x) + J_{a2} + J_t) \left(\frac{r_1}{r_t}\right)^2 \tag{2.11}$$

2.2 Forces and torques

Left to its own devices, the tape-spring would quickly unfurl, releasing the energy stored in the coil. The guide elements in the implementation direct this release of energy, while the motors control its rate of release.
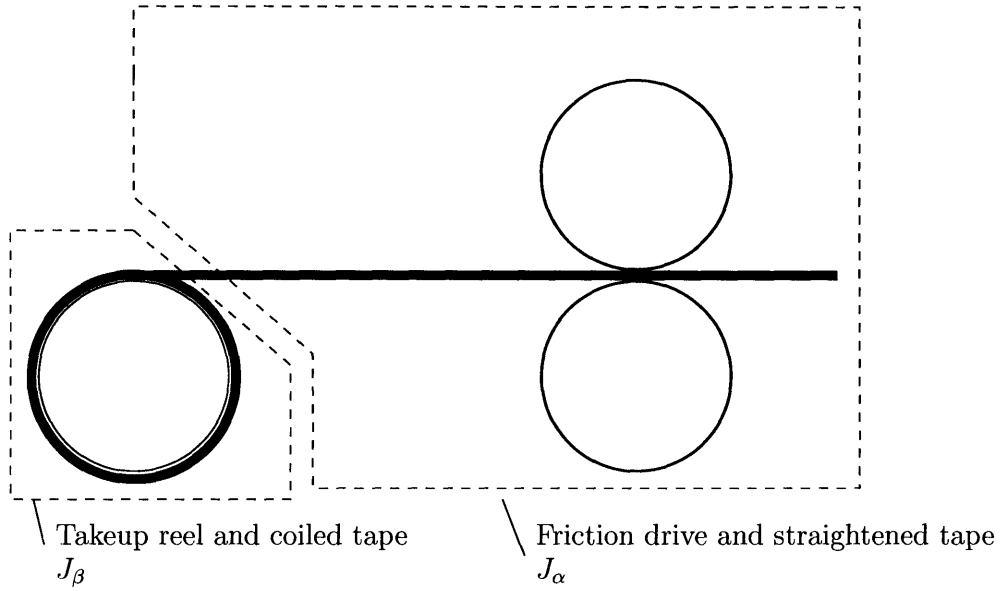
Figure 2-2: A convenient grouping of the system inertias

2.2.1 Tape-spring

Rimrott's work [10] includes an evaluation of the strain energy stored in a coiled STEM as a function of the coiled length $l - x$ which in the current nomenclature is

$$V_c = \frac{E}{1 - \nu^2} \frac{\phi t^3 (l - x)}{12 d_0} \left(1 + \frac{d_0^2}{4 r_t^2} + \frac{2 \nu d_0}{2 r_t}, \right) \tag{2.12}$$

where E and ν are the elastic modulus and Poisson's ratio for the tape spring material, t the thickness of the tape, d_0 is the diameter of the cross section and ϕ the number of radians covered by the cross section of the tape, as shown in Figure 2-3. The force associated with the impetus to uncoil is

$$F_c = -\frac{\partial V_c}{\partial x} = \frac{E}{1 - \nu^2} \frac{\phi t^3}{12 d_0} \left(1 + \frac{d_0^2}{4 r_t^2} + \frac{2 \nu d_0}{2 r_t} \right) \tag{2.13}$$

Substituting $\theta_t = \frac{x}{r_t}$ into Equation (2.12) and solving $\tau_{c_t} = -\frac{\partial V}{\partial \theta}$ in the manner of Equation (2.13), results in expressions for τ_{c_t}, the torque from the coil on the takeup
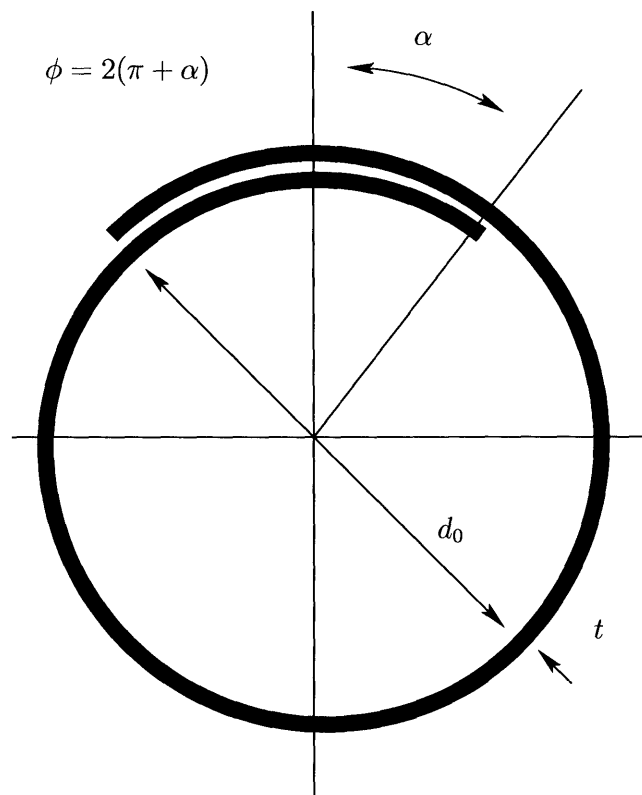
22

Figure 2-3: End view of curled STEM

reel, and τ_c, the effective torque from the coil on the whole system:

$$\tau_{c_t} = \frac{E}{1-\nu^2}\frac{\phi t^3 r_t}{12 d_0}\left(1 + \frac{d_0^2}{4 r_t^2} + \frac{2\nu d_0}{2 r_t}\right) \tag{2.14}$$

$$\tau_c = \frac{E}{1-\nu^2}\frac{\phi t^3 r_1}{12 d_0}\left(1 + \frac{d_0^2}{4 r_t^2} + \frac{2\nu d_0}{2 r_t}\right). \tag{2.15}$$

Tape uncoiling torque
τ_{c_t}

Tension
T

Torque from drive motor
τ_1

Backtorque from tensioning motor
τ_2
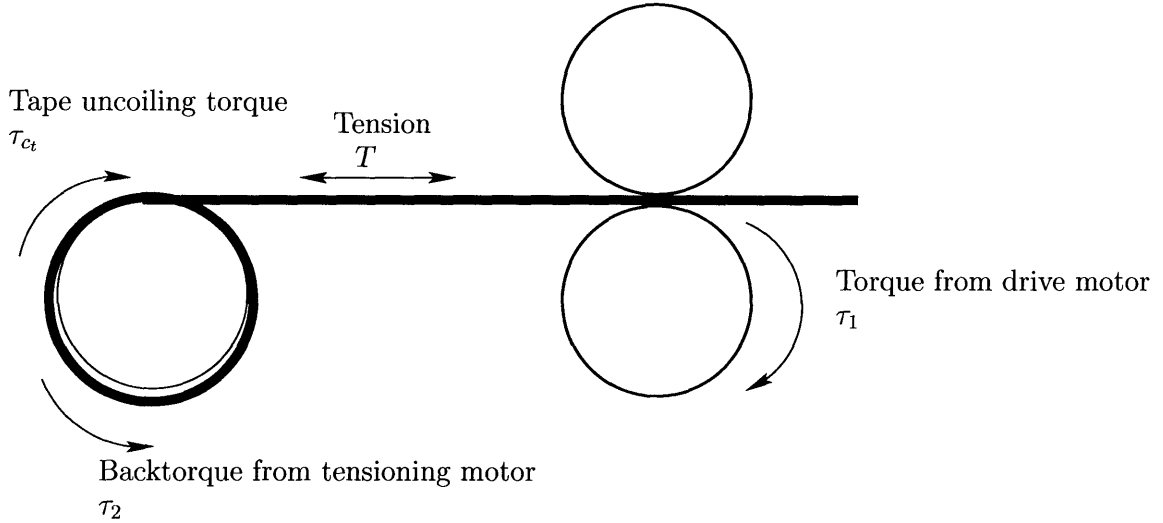
Figure 2-4: Torques and forces in the system

2.2.2 Back torque

An area not covered by Rimrott is rewrapping of the tape-spring during retraction. If the takeup reel were to be left idle, the tape-spring would not wrap neatly around it as the pinch rollers fed the STEM back into the magazine. Instead, the tape would form a loose spiral out from the reel. At the very least, this behavior would play havoc with the moment of inertia of the coil. Further, the loose spiral form becomes a spring coupling between the drive wheel and the takeup reel, introducing a second degree of freedom and the possibility for unplanned resonances to appear.

This detrimental decoiling can occur when the position of the takeup reel is more positive than that of the drive motor. The coils are unable to take a compressive load and will peel off as seen in Figure 2-5, finding a new low-energy state. For ease

of discussion, avoiding compressive forces at the coil juncture will be referred to as maintaining a tension T between the coil and the pinch rollers, bearing in mind that some component of this force is contributed by the strain in the ploy section. The magnitude of the necessary tension as a function of the system state is found below, but for the present, the minimum tension required in any state will be referred to as T_m.
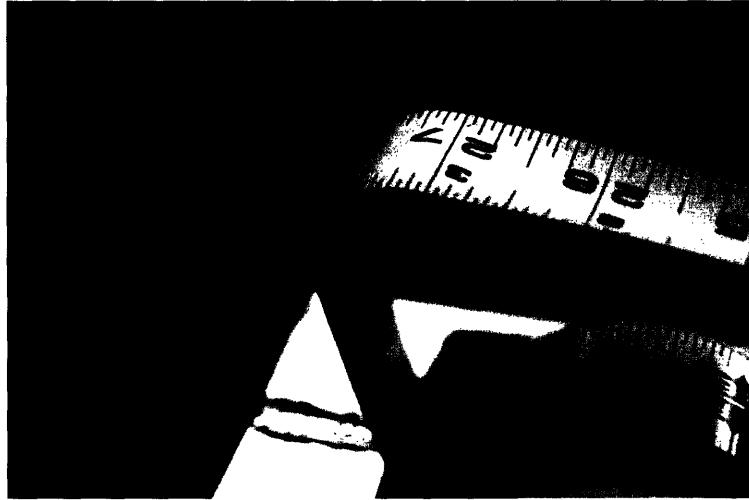
Figure 2-5: Decoiling failure arrested in mid process; tape should leave coil at the 36.5 inch mark.

A simple, though perhaps not the most power efficient, way of maintaining $T > T_m$ is to include in the controller a hard limit on the maximum magnitude of acceleration in the negative direction, thus limiting the acceleration $\ddot{x}$ to

$$\ddot{x} > -a_{max}, \tag{2.16}$$

where a_{max} is the maximum allowable acceleration of the system and is thus a design point related to the desired speed of response. With this acceleration limit in place, the motor on the takeup reel can be set to exert a constant torque sufficient to provide $T > T_m$ for all accelerations in the allowable range. As the equation of motion for

the reel and the spring coiled around it, with Motor 2 providing a torque τ_2, is

$$\frac{J_2(x)}{r_t}\ddot{x} = Tr_t + \tau_{c_t} + \tau_2, \qquad (2.17)$$

when $\ddot{x} = -a_{max}$,

$$\tau_2 = -\left[a_{max}\left(\frac{J_2(x)}{r_t}\right) + Tr_t + \tau_{c_t}\right]. \qquad (2.18)$$

Equation (2.18) can be considered optimized when τ_2 is set at the smallest value for which the necessary tension is maintained. As T must be at least T_m and the greatest value for $J_2(x)$ is

$$J_2(0) = M_T r_t^2 + J_{a2} + J_t, \qquad (2.19)$$

we arrive at an expression for the backtorque needed to control the wrapping of the tape-spring:

$$\tau_2 = -\left[a_{max}\left(\frac{M_T r_t^2 + J_{a2} + J_t}{r_t}\right) + Tr_t + \tau_{c_t}\right]. \qquad (2.20)$$

2.2.3 Driving torque

With the backtorque found, we now turn our attention to the driving torque. As the three net torques on the system (not counting external loads, addressed below) are from the drive motor, τ_1, the back motor, τ_2 and the coil, τ_c, the equation of motion for the tape-spring is

$$M_M\ddot{x} = \frac{\tau_1}{r_1} + \frac{\tau_2 + \tau_c}{r_t}. \qquad (2.21)$$

For control purposes, τ_1 can be broken down into a constant component balancing the back torque and a varying part that provides the impetus for motion and responds to a control signal:

$$M_M\ddot{x} = \frac{\tilde{\tau}_1}{r_1} + \frac{\bar{\tau}_1}{r_1} + \frac{\tau_2 + \tau_c}{r_t}. \qquad (2.22)$$

Setting

$$\bar{\tau}_1 = -(\tau_2 + \tau_c)\frac{r_1}{r_t} \qquad (2.23)$$

26

simplifies the equation of motion to

$$M_M \ddot{x} = \frac{\tilde{\tau}_1}{r_1}, \tag{2.24}$$

describing a system for which it is trivial to set the point anywhere in the range (with the center being an obvious choice) and to which standard control methods may be applied.

For the system to be able to achieve acceleration $\ddot{x} = a_{max}$, the variable torque must be able to achieve

$$\tilde{\tau}_1 = (M_M \ddot{x} + L)r_1, \tag{2.25}$$

where L_{max} is the maximum load under expected conditions, and thus the motor must be able to supply torque

$$\tau_1 = (M_M \ddot{x} + L_{max})r_1 - (\tau_2 + \tau_c)\frac{r_1^2}{r_t}. \tag{2.26}$$

Chapter 3

Full Model

While existing analyses of tape-springs in general and the STEM in particular make use of the simplification that the tape winds around the drum at the constant radius of r_t, there is little consideration of the extent to which this approximation is appropriate. An evaluation of how the actual inertias and forces compare to those found in Chapter 2 follows.

3.1 Model differences

In taking into account the changes in radius, the chief change is to move from regarding the coil as a thin ring of radius r_t to regarding it as a thick ring with inner radius r_t and outer radius r_o as in Figure 3-1. This outer radius can be found as the radius of the circle with area equal to sum of the cross sections of the takeup reel and the coil,

$$\pi r_o^2 = \pi r_t^2 + A_{\text{coil}}.$$ (3.1)

As

$$A_{\text{coil}} = t(l - x),$$ (3.2)

the outer radius of the coil is seen to be

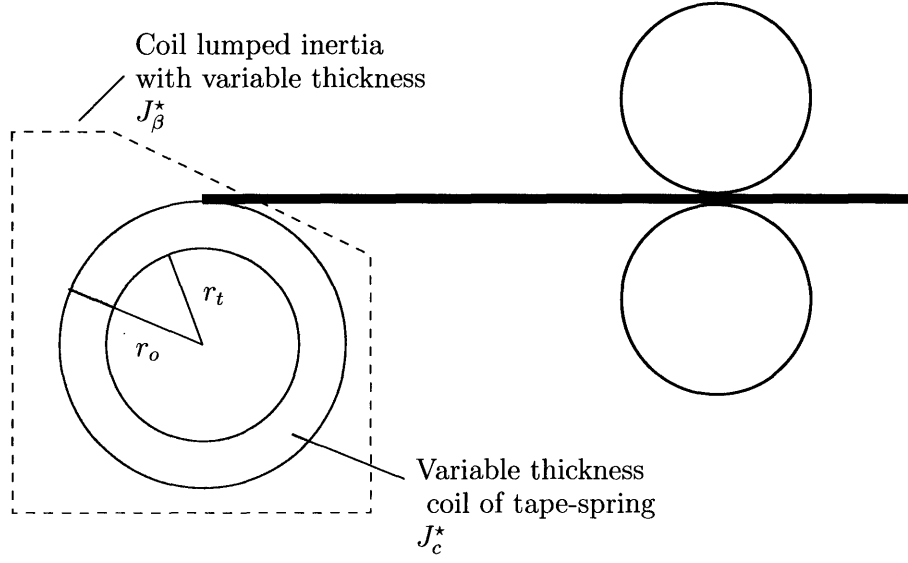$$r_o^2 = r_t^2 + \frac{t(l - x)}{\pi}.$$ (3.3)

Figure 3-1: New inertias with variable wrapping diameter

3.1.1 Inertias

The linear inertia term remains the same, but the moment of inertia of the coil around its center must be found using the equation for a thick ring,

$$J_{\text{ring}} = \frac{1}{2}m(r_{\text{in}}^2 + r_{\text{out}}^2). \tag{3.4}$$

The new moments of inertia of the coil, $J_c^\star$, the takeup side of the mechanism, $J_\beta^\star$, and the whole system, $J_J^\star$, are thus found by combining Equations (3.3) and (3.4):

$$J_c^\star = \frac{1}{2}\rho(l-x)\left(2r_t^2 + \frac{t(l-x)}{\pi}\right) \tag{3.5}$$

$$J_\beta^\star = \left(\frac{1}{2}\rho(l-x)\left(2r_t^2 + \frac{t(l-x)}{\pi}\right) + J_t\right)\frac{r_1^2}{r_t^2 + \frac{t(l-x)}{\pi}} \tag{3.6}$$

$$J_J^\star = \left(\frac{1}{2}\rho(l-x)\left(2r_t^2 + \frac{t(l-x)}{\pi}\right) + J_t\right)\frac{r_1^2}{r_t^2 + \frac{t(l-x)}{\pi}} + J_\alpha \tag{3.7}$$

3.1.2 Coil Force

As the coil releases energy from its outermost layer, r_o substitutes for r_t in Equations (2.14) and (2.15), the new terms for these torques, $\tau_{c_t}^\star$ and $\tau_c^\star$ are

$$\tau_{c_t}^\star = \frac{E}{1-\nu^2} \frac{\phi t^3 \sqrt{r_t^2 + \frac{t(l-x)}{\pi}}}{12d_0} \left(1 + \frac{d_0^2}{4(r_t^2 + \frac{t(l-x)}{\pi})} + \frac{2\nu d_0}{2\sqrt{r_t^2 + \frac{t(l-x)}{\pi}}} \right) \tag{3.8}$$

$$\tau_c^\star = \frac{E}{1-\nu^2} \frac{\phi t^3 r_1}{12d_0} \left(1 + \frac{d_0^2}{4(r_t^2 + \frac{t(l-x)}{\pi})} + \frac{2\nu d_0}{2\sqrt{r_t^2 + \frac{t(l-x)}{\pi}}} \right). \tag{3.9}$$

3.2 Comparison of models

Examination of the plots of the functions found above, Figures 3-2 and 3-3, show that the effective mass and force are actually less than those predicted by the first order model, converging at the extreme extension, $x = l$. While it is intuitive that the increased bend radius at low extensions would decrease the force exerted by the coil, the decrease in effective inertia with an increased radius is less so. It can most succinctly be explained as an effect of the tape matching speeds with the outside of the coil, causing inner wraps to move more slowly than the straightened section. Another view is that the transmission ratio from the drive wheel to the motor is more sensitive to changes in radius than is the inertia of the coil.

An interesting ramification of the wrapping process is that a shorter STEM with all other characteristics equal will match up with the far right hand side of Figures 3-2 and 3-3 and increased length will add to its range to the left and down the curve.

3.3 Simulations

While a complete analysis of the dynamic behavior of the more complex model found above is beyond the scope of this thesis, numerical methods were used to model specific instances of STEM implementation. The results of these simulations are
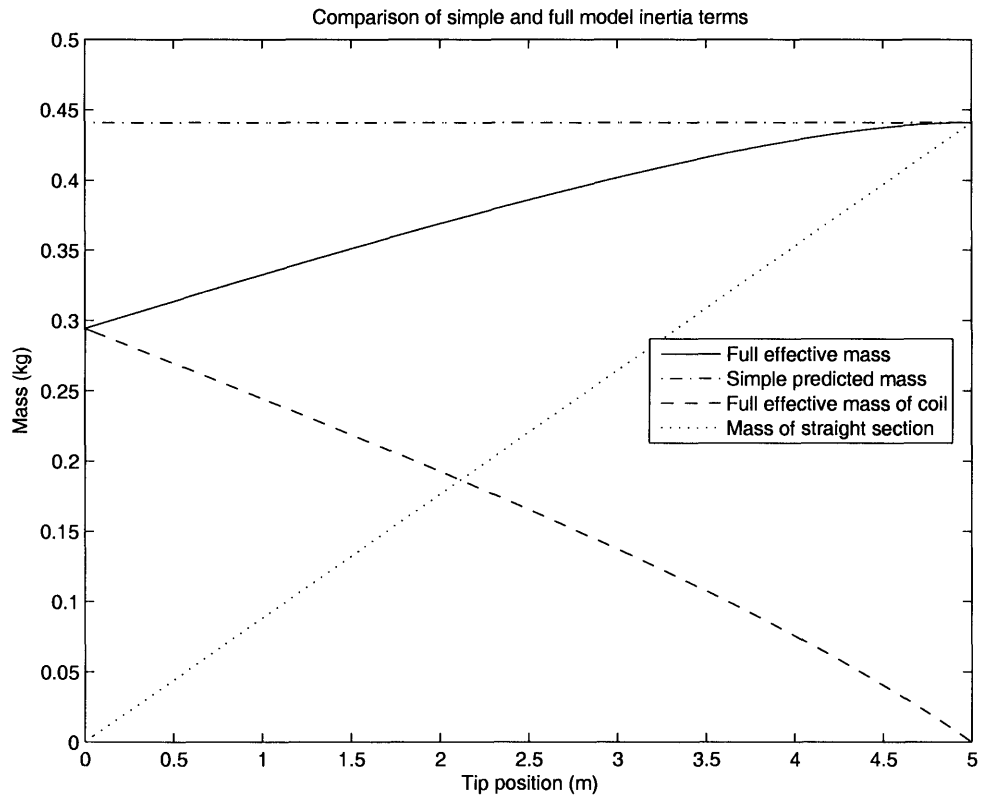
Figure 3-2: Comparison of the masses predicted by the first order and detailed models.
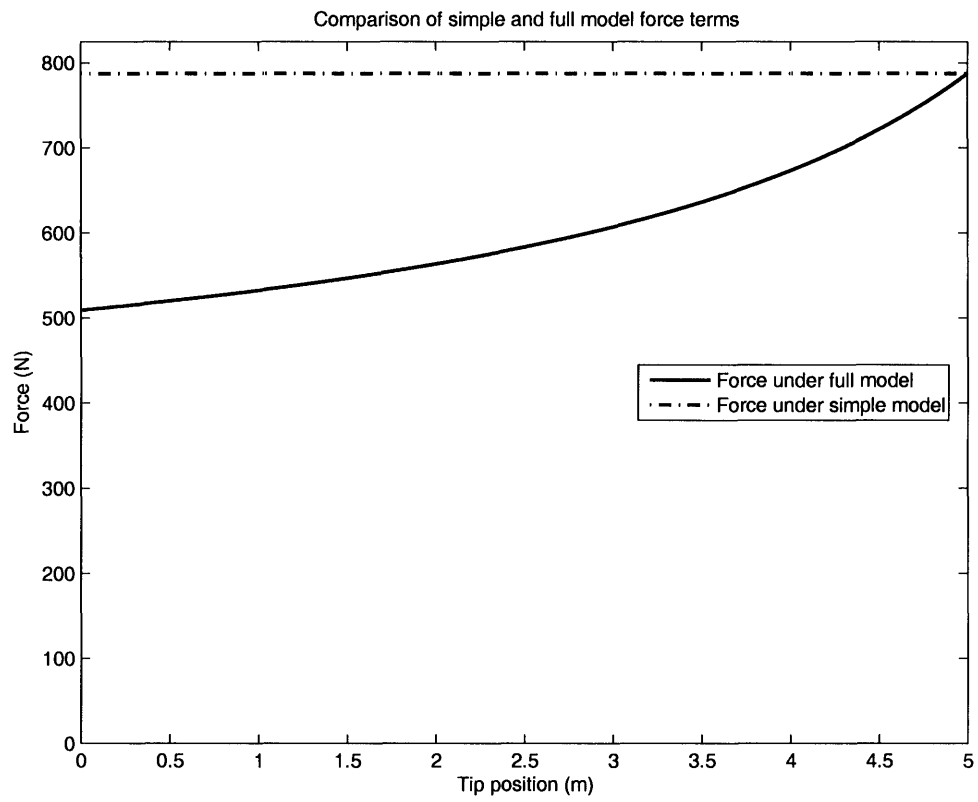
Figure 3-3: Comparison of the uncoiling force predicted by the first order and detailed models.

analyzed for any trends providing a starting point for future investigations.

The numerical investigations were carried out in Matlab™. Simulink™, Matlab's graphical programming tool for solving differential equations provided a platform for testing the model's step responses under various conditions, the results of which were fed into data extraction scripts to evaluate the differences in response at different conditions. For each situation, the simple plant model and the full model were placed identical feedback loops and driven off the same input. Also in each situation, the same feedback loops were applied to the plant models, but with minor loops wrapped around the plants. For all cases in which the gain was not explicitly varied, it was scaled with the mass of the ideal plant, such that the simulations were normalized to the ideal plant having dominant oscillating poles at $\pm 45°$.

In Figures 3-4 and 3-5 appear the results of applying a step input to a spring steel STEMs covering a range of lengths. The steady-state error, shown in Figure 3-4 drops off as the STEM length is increased, an effect likely due to the increase in gain with STEM length. While the gain and mass rise together with length, maintaining consistency of dynamic behavior, the gain rises much faster than the difference between the ideal and actual forces.

Meanwhile, the overshoot increases with the length of the STEM. In this case, the hypothesis for future work is that, by Figure 3-2, a STEM is proportionally more underweight the longer it is. Being underweight effectively increases the system gain and pushes the roots further out along the asymptotes for faster response but decreased stability. If this is the case, it accounts for the slowing in the overshoot rise as the F_c levels off.

As might be expected, increasing the effective mass of the rotors in proportion to the effective mass of the tape-spring decreases the overshoot error as in Figure 3-6. This effect has the straightforward explanation that as the rotors become more dominant in the inertia term, the effect of the variation from the tape-spring becomes less significant to the net inertia.

The effect of moving the poles of the closed loop system around was investigated with a simulation, but no trend was found between the variations in gain and any

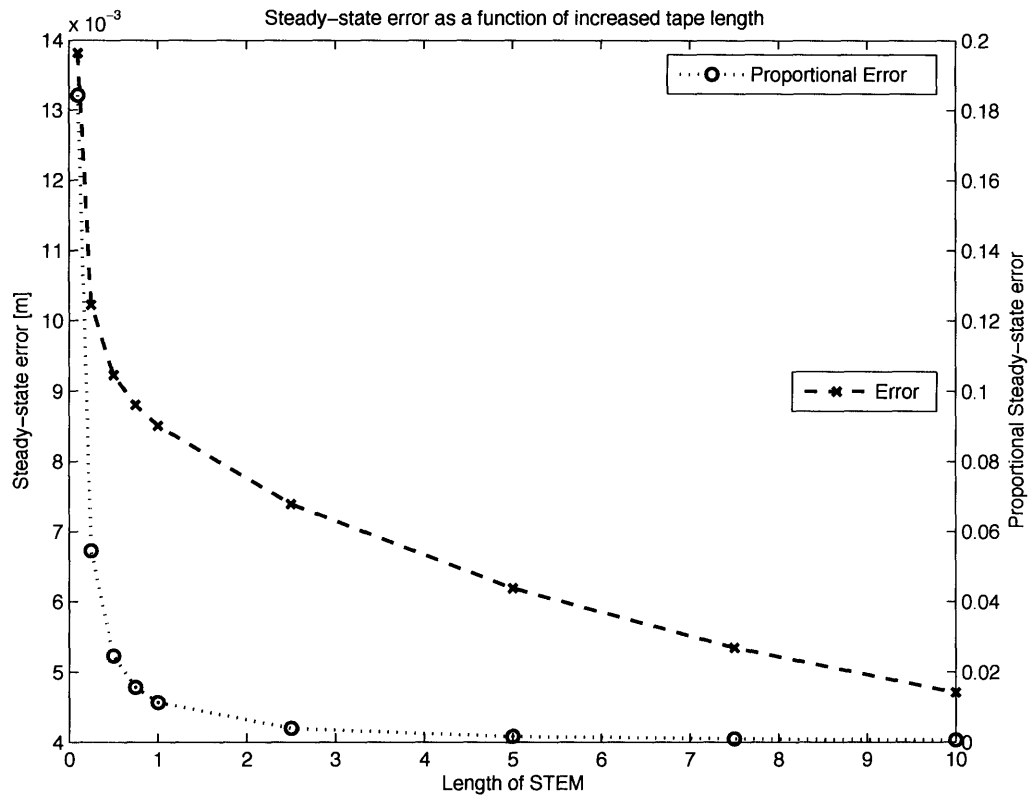differences between the ideal model and the full model.

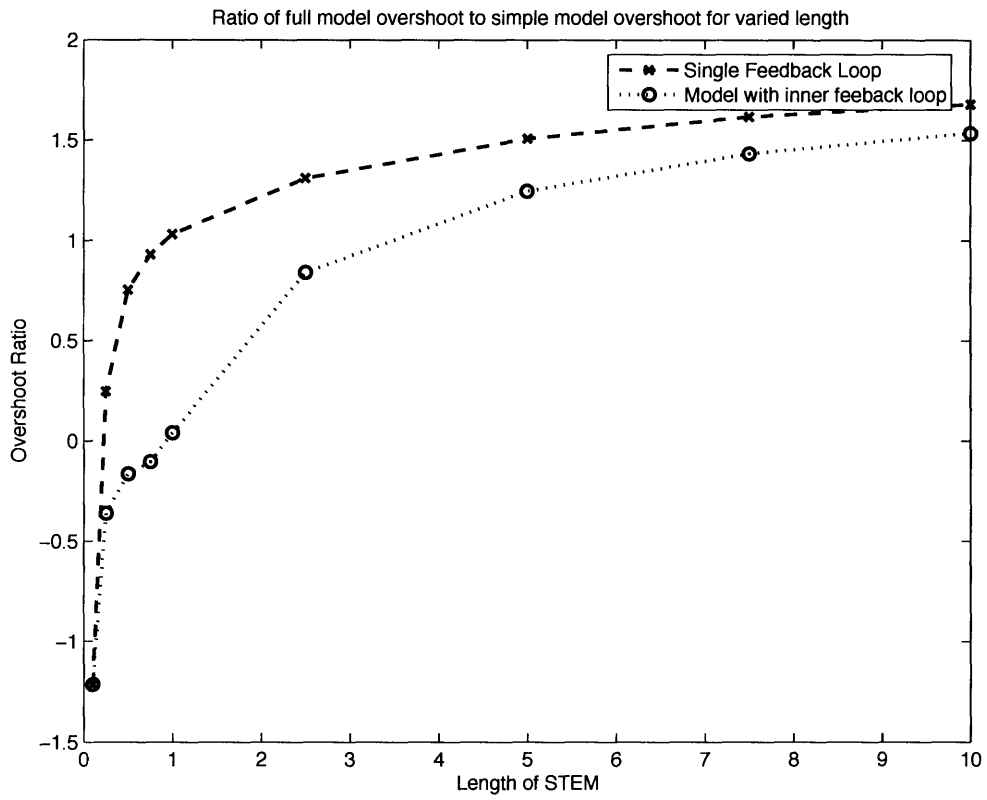Figure 3-4: Steady state errors across varying STEM length

Figure 3-5: Ratios of peak overshoots across varying STEM length
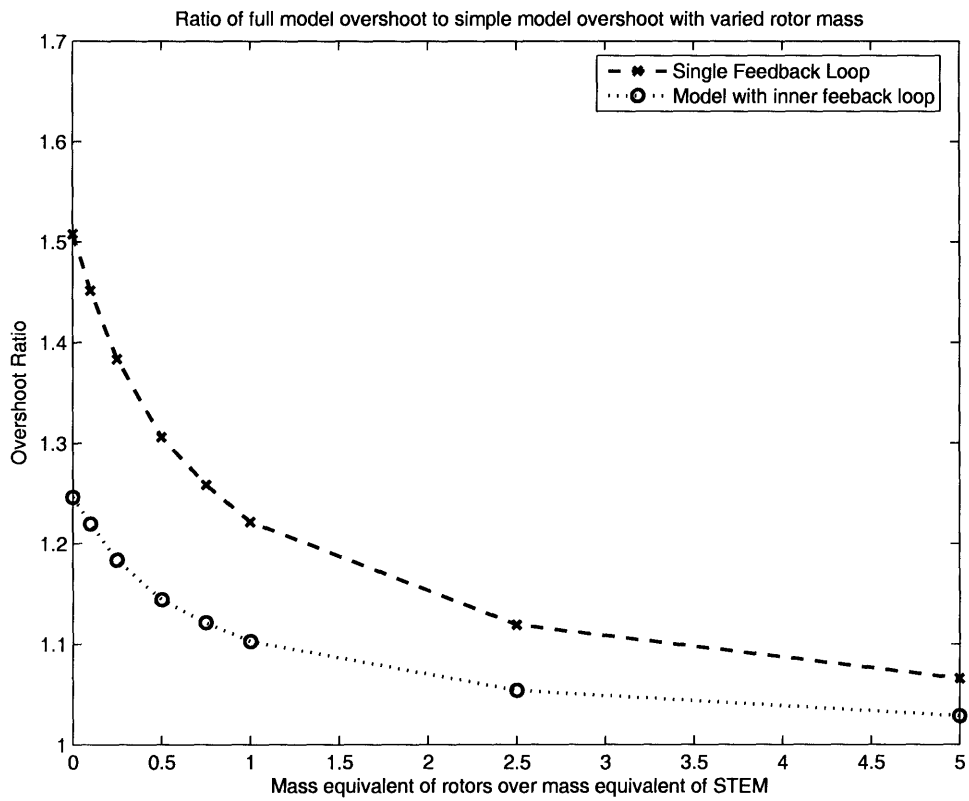
Figure 3-6: Ratios of peak overshoots with increasing rotor mass

Chapter 4

Conclusions and Future Work

This thesis has presented a framework for modeling long-stroke linear actuators based on the STEM. In surveying the various rotary-to-linear transmission elements used in practice, it provides a basis for choosing the STEM as a transmission element. New work was done in adapting the published examinations of the STEM to a form suitable for use in a feedback control system. Further, the body of literature was expanded upon with a complete solution for the inertias and forces from stored energy for a tape-spring stored on a reel.

The model for an actuator found in Chapter 2 is valid for most envisioned implementations. Much of the theory behind it has been well documented and experimentally confirmed in prior work. Where prior work was not publicly available, such as in the maintenance of tight wrapping around the spool, new theories have been advanced and studied through simulation. The chief difference between versions of the STEM discussed in earlier papers and the implementation discussed here is that most earlier discussions focus on using the stored energy in the coiled tape-spring as the source of motive force, whereas this implementation counters the natural unwinding force of the spring, then applies motive forces to the rigid extension section. One very useful feature of this model is that it can be made to act as a pure inertia when incorporated into a feedback system.

With better computational resources today than were available in 1965 during early development of the STEM, it became feasible to evaluate Rimrott's conjecture

that for expected lengths the simple forms of the equations for the force on and inertia of a coiled STEM could be used without consideration of the changes in wrapping diameter at different extensions. The simulations carried out showed that appropriate and implementable control schemes maintain the expected settling time but add to the expected overshoot.

4.1 Future work

Several avenues exist for future work on the described actuator design. Of most interest would be a working implementation of the actuator to experimentally verify the model. Experimental results will also highlight damping present in the system for inclusion into an even more complete model, along with a way of characterizing any hysteresis between extension and retraction. Work at Cambridge University is currently being done on bi-stable tape-springs which have an activation energy associated with moving into configurations between the flat and curved regimes and thus don't have a tendency to fly open. If these springs can be manufactured as STEMs, a path is opened for variations on the present actuator that require much smaller motors or negator springs. Alternately, the bi-stable springs may prove to be useful enough over traditional versions that a zippered actuator made of them becomes the most viable option. One additional area of investigation would be in the scaling of tape-spring linear actuators. Current models are generally in the range of 1" − 20", and producing a long-stroke actuator for lab bench or smaller applications has potential.

Appendix A

Computer models

Various computer models and programs which were incorporated into this thesis.

A.1 Simulink Block Diagrams

Figure A-1 has three subsystems. The variable mass is always filled by the block in Figure A-2. Depending on the test, the ideal and full loop blocks are filled by those in Figures A-3 and A-5 or A-4 and A-6 respectively.
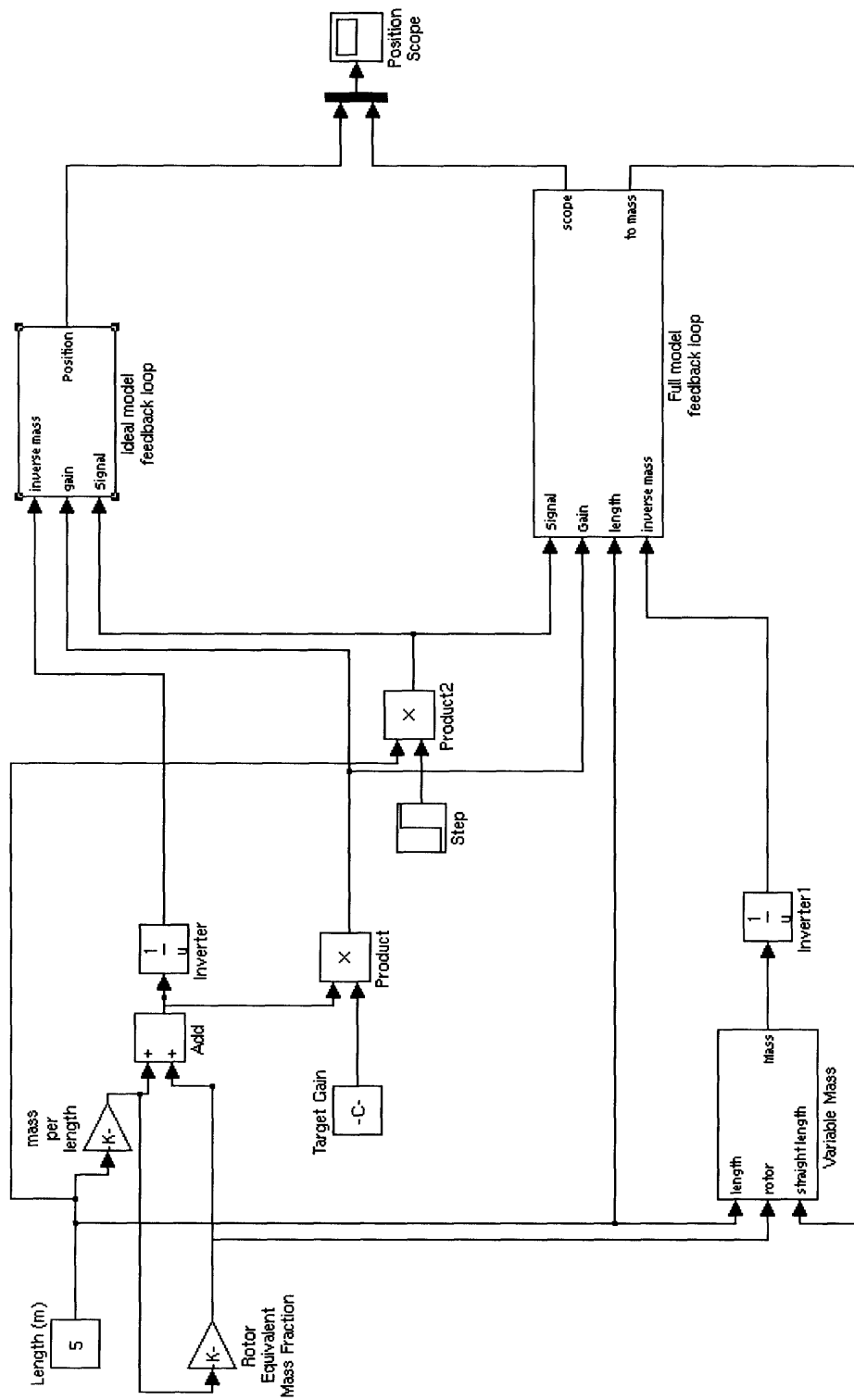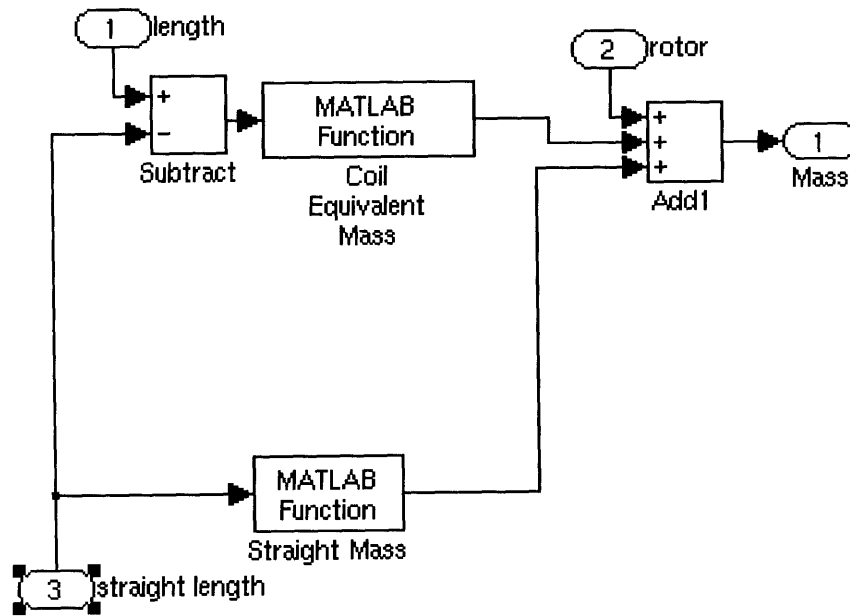
Figure A-1: Main block diagram for simulation.

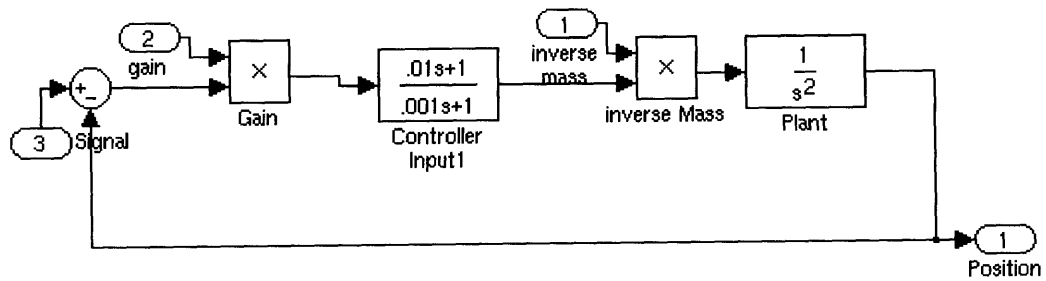Figure A-2: Subsystem for calculating variable mass.

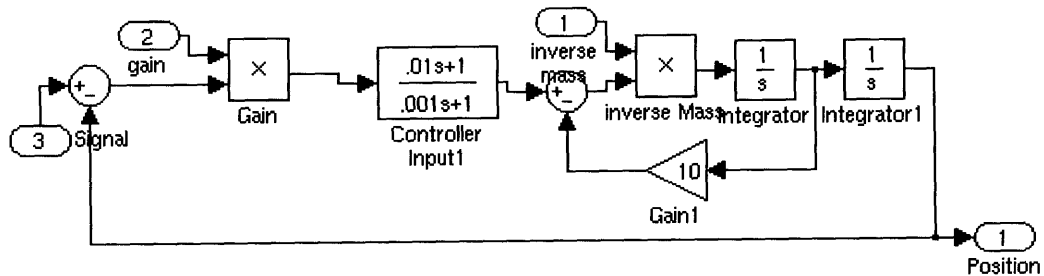Figure A-3: Plant and compensator for simple model.

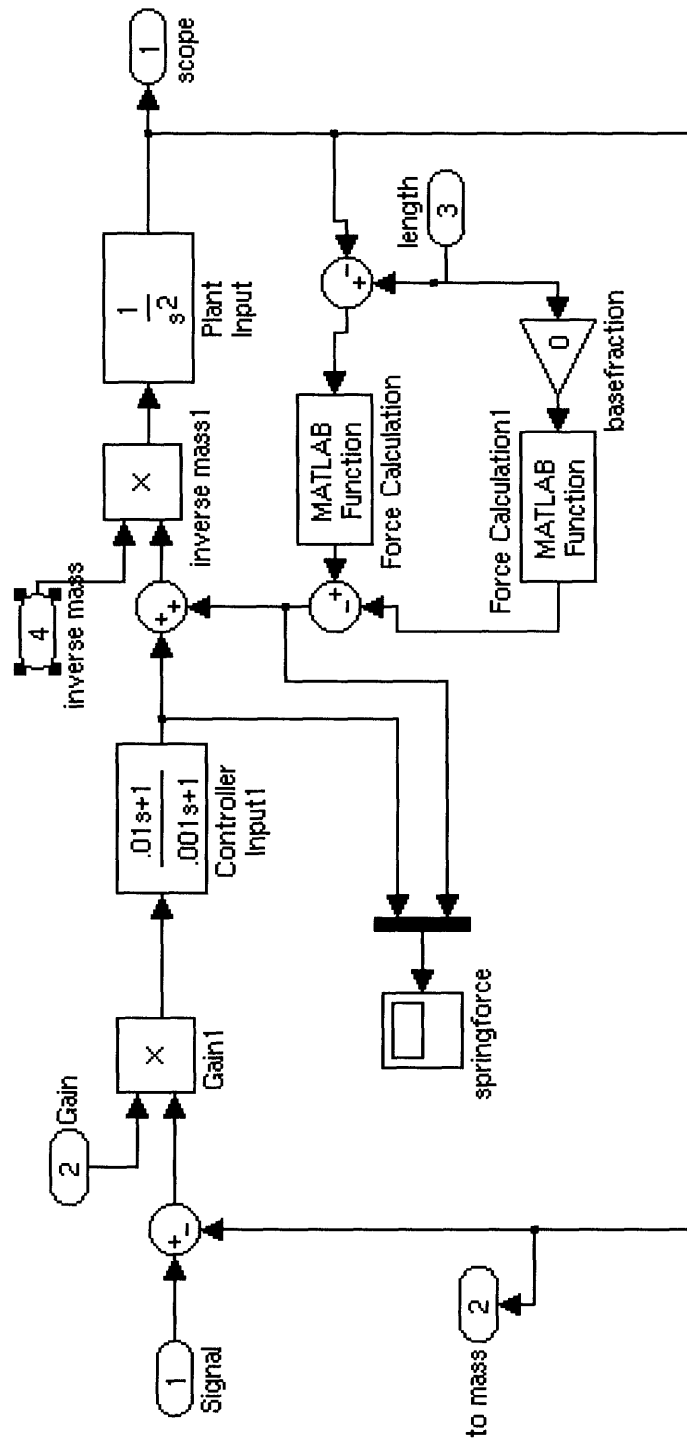Figure A-4: Plant and compensator for simple model with minor loop feedback.

41

Figure A-5: Plant and compensator for full model.
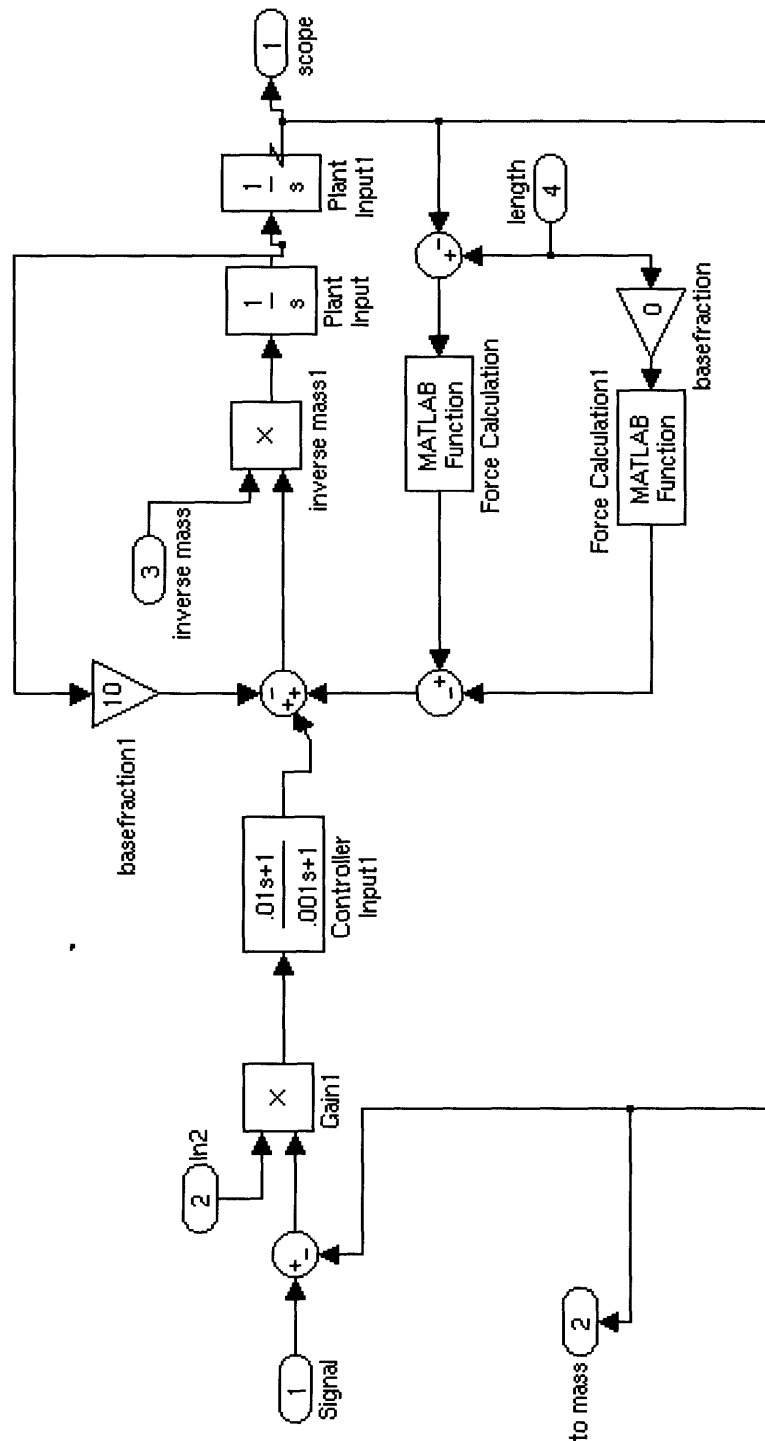
Figure A-6: Plant and compensator for full model with minor loop feedback.

A.2 Functions called by blocks

A.2.1 Mass of straightened tape

```
function [M_strict] = TapeM(x)

%Parameters of STEM
rho=7.85e3;                            %density of tape material
t=1.25e-4;                             %thickness of strip in flat form
l=1;                                   %length of tape
D=.02;                                 %diameter of tube
alpha=77.5;                            %half-overlap
E=210e9;                               %Young's Modulus of material
nu=.3;                                 %Poisson's Ration of material


%derived parameters
w=((360+2*alpha)/360)*pi*D;             %width of flat tape
gmma=1+alpha/pi;                        %intermediate term in spring equation


J_strict = Jfind(x,rho,t,l,D,alpha,E,nu,w,gmma);
M_strict = Mfind(x,rho,t,l,D,alpha,E,nu,w,gmma);
R_o_strict_squared = Ro2find(x,rho,t,l,D,alpha,E,nu,w,gmma);

Meq = Mnetfind(J_strict,M_strict,R_o_strict_squared);


function [Jstrict] = Jfind(x,rho,t,l,D,alpha,E,nu,w,gmma)
%finds strict solution of coil inertia for a given position
    Jstrict = rho*t*w*(l-x)*(D^2/4+(t*(l-x))/(2*pi));

function [Mstrict] = Mfind(x,rho,t,l,D,alpha,E,nu,w,gmma)
%finds mass of sliding portion as for given position
    Mstrict = rho*t*w*x;

function [Ro2] = Ro2find(x,rho,t,l,D,alpha,E,nu,w,gmma)
%finds the outer radius of the coil for given position
    Ro2 = D^2/4+(t*(l-x))/pi;

function [Mstrictnet] = Mnetfind(J,M,Ro2)
%finds the net mass seen anywhere along the formed tube
    Mstrictnet = J/Ro2+M;
```

44

A.2.2 Equivalent mass of coiled tape

```
function [J_strict_mequiv] = TapeMeqJ(lmx)


%Parameters of STEM
rho=7.85e3;                          %density of tape material
t=1.25e-4;                           %thickness of strip in flat form
l=1;                              %length of tape
D=.02;                               %diameter of tube
alpha=77.5;                          %half-overlap
E=210e9;                             %Young's Modulus of material
nu=.3;                               %Poisson's Ration of material



%derived parameters
w=((360+2*alpha)/360)*pi*D;           %width of flat tape
gmma=1+alpha/pi;                     %intermediate term in spring equation



J_strict = Jfind(lmx,rho,t,l,D,alpha,E,nu,w,gmma);
% M_strict = Mfind(x,rho,t,l,D,alpha,E,nu,w,gmma);
R_o_strict_squared = Ro2find(lmx,rho,t,l,D,alpha,E,nu,w,gmma);
%
% Meq = Mnetfind(J_strict,M_strict,R_o_strict_squared);
%
J_strict_mequiv= Jstrictmequivfind(J_strict, R_o_strict_squared);



function [Jstrict] = Jfind(lmx,rho,t,l,D,alpha,E,nu,w,gmma)
%finds strict solution of coil inertia for a given position
    Jstrict = rho*t*w*(lmx)*(D^2/4+(t*(lmx))/(2*pi));

% function [Mstrict] = Mfind(x,rho,t,l,D,alpha,E,nu,w,gmma)
% %finds mass of sliding portion as for given position
%       Mstrict = rho*t*w*x;
%
 function [Ro2] = Ro2find(lmx,rho,t,l,D,alpha,E,nu,w,gmma)
 %finds the outer radius of the coil for given position
      Ro2 = D^2/4+(t*(lmx))/pi;

% function [Mstrictnet] = Mnetfind(J,M,Ro2)
% %finds the net mass seen anywhere along the formed tube
%       Mstrictnet = J/Ro2+M;
%
```

```
function [Jstrictmequiv] = Jstrictmequivfind(J,Ro2)
%finds the net inertia seen at the drive axle of the spool
Jstrictmequiv = J/Ro2;
```

A.2.3   Unwinding force of coil

```
function [force] = TapeF(Y)


%Parameters of STEM
rho=7.85e3;                              %density of tape material
t=1.25e-4;                               %thickness of strip in flat form
l=5;                                   %length of tape
D=.02;                                   %diameter of tube
alpha=77.5;                              %half-overlap
E=210e9;                                 %Young's Modulus of material
nu=.3;                                   %Poisson's Ration of material


%derived parameters
w=((360+2*alpha)/360)*pi*D;               %width of flat tape
gmma=1+alpha/pi;                          %intermediate term in spring equation


% function [F] = Ffind(x)
%Finds the unrolling force as a function of x
%       global rho t l D alpha E nu w gmma;
%     Y=l-x
    K=(E*gmma*pi*t^3)/((1-nu^2)*6*D);
    a=D^2;
    b=2*nu*D;
    f=D^2;
    c=4*t/pi;
    H=f+c*Y;
    force=K*(1+a/(H)+b/(H)^.5);
```

A.3   Other programs

A.3.1   Extraction and plotting code for Simulink Results

```
function lengthextract

headers=[
```

```
    %length, rotor percentatge, gain, zero, pole
    .1   0   4.93e4   .01 .001
    .25  0   4.93e4   .01 .001
    .5   0   4.93e4   .01 .001
    .75  0   4.93e4   .01 .001
    1    0   4.93e4   .01 .001
    2.5  0   4.93e4   .01 .001
    5    0   4.93e4   .01 .001
    7.5  0   4.93e4   .01 .001
    10   0   4.93e4   .01 .001
    ];

load lengthdata2


lengthexperiment{1,2}.signals.values(1,1)

[final peak sserror twopsettle]=thesiscare(lengthexperiment);

for i=1:4,
    cbase=(((floor((i+1)/2))*2)-1);
    osratio(:,:,i)=(peak(:,:,i)-final(:,:,cbase))./(peak(:,:,1)...
        -final(:,:,cbase));
    sserrorprc(:,:,i)=sserror(:,:,i)./final(:,:,cbase);
    settleprc(:,:,i)=twopsettle(:,:,i)./twopsettle(:,:,cbase);
end


figure(2)
subplot(2,1,1)
plot(headers(:,1), osratio(:,1,2),'x', headers(:,1),...
    osratio(:,1,4), 'o')
subplot(2,1,2)
plot(headers(:,1), osratio(:,2,2),'s', headers(:,1),...
    osratio(:,2,4), 'd')
title('Peak Deviation with Tape Length')

figure(3)
subplot(2,1,1)
plot(headers(:,1), sserrorprc(:,1,2),'x', headers(:,1),...
    sserrorprc(:,1,4), 'o')
subplot(2,1,2)
plot(headers(:,1), sserrorprc(:,2,2),'s', headers(:,1),...
    sserrorprc(:,2,4), 'd')
```

```
title('Fraction of steady state error with Tape Length')

figure(4)
subplot(2,1,1)
plot(headers(:,1), settleprc(:,1,2),'x', headers(:,1),...
    settleprc(:,1,4), 'o')
subplot(2,1,2)
plot(headers(:,1), settleprc(:,2,2),'s', headers(:,1),...
    settleprc(:,2,4), 'd')
title('Settling time deviation with tape length')

figure(5)
subplot(2,1,1)
plot(headers(:,1), sserror(:,1,2),'x', headers(:,1), sserror(:,1,4), 'o')
subplot(2,1,2)
plot(headers(:,1), sserror(:,2,2),'s', headers(:,1), sserror(:,2,4), 'd')
title('absolute steady state error with Tape Length')


figure(17517)
[AX,H1,H2]=plotyy(headers(:,1), sserror(:,1,2), headers(:,1),...
    sserrorprc(:,1,2))
set(H1,'LineStyle','--','LineWidth',1.5,'Marker','x');
set(H2,'LineStyle',':','LineWidth',1.5,'Marker','o');
set(get(AX(1),'Ylabel'),'String','Steady-state error [m]');
set(get(AX(2),'Ylabel'),'String','Proportional Steady-state error');
%axis(AX(2), [0 10 -.6 .1]);
xlabel('Length of STEM')
title('Steady-state error as a function of increased tape length')
legend(H1, 'Error','Location','East')
legend(H2, 'Proportional Error','Location','NorthEast')
print sserrorfig -depsc

figure(17217)
plot(headers(:,1), osratio(:,1,2),'x','LineStyle','--','LineWidth',1.5)
hold on
plot(headers(:,1), osratio(:,1,4),'o', 'LineStyle',':','LineWidth',1.5)
hold off
title...
('Ratio of full model overshoot to simple model overshoot for varied length')
xlabel('Length of STEM')
ylabel('Overshoot Ratio')
legend('Single Feedback Loop','Model with inner feeback loop')
print overshotfig -depsc
```

```
function [final peak sserror twopsettle] = thesiscare(dataset)

%data columns are ideal,full plant model, ideal, full plant model with
%closed internal loop


[MM, NN]=size(dataset);


for i=1:MM
    for n=1:NN
        for q=[1:4]
            for p=0:length(dataset{i,n}.signals.values)-1
%                 i
%                 n
%                 q
%                 p
                if abs((dataset{i,n}.signals.values(end-p,q)- ...
                        dataset{i,n}.signals.values(end,q))/...
                        dataset{i,n}.signals.values(end,q)) >= .03
                    %.03 accounts for offset in initial value
                    twopsettle(i,n,q)=dataset{i,n}.time(end-p,1)-1;
                    break
                end
            end

            if n==1
                peak(i,n,q) = max(dataset{i,n}.signals.values(:,q));
            elseif n==2
                peak(i,n,q) = min(dataset{i,n}.signals.values(100:end,q));
            end
            final(i,n,q) = dataset{i,n}.signals.values(end,q);
            sserror(i,n,q) = dataset{i,n}.signals.values(end,1)...
                -dataset{i,n}.signals.values(end,q);


        end

    end
end
```

A.3.2 STEM modeling code

```
function stemlinearization
```

```matlab
%This function simulates the dynamic response of a STEM device
%It compares various linearizations with a complete model

global rho t l D alpha E nu w gmma;        %makes material parameters global


%Parameters of STEM
rho=7.85e3;                                %density of tape material
t=1.25e-4;                                 %thickness of strip in flat form
l=5;                                   %length of tape
D=.02;                                     %diameter of tube
alpha=77.5;                                %half-overlap
E=210e9;                                   %Young's Modulus of material
nu=.3;                                     %Poisson's Ration of material


%derived parameters
w=((360+2*alpha)/360)*pi*D;                %width of flat tape
gmma=1+alpha/pi;                           %intermediate term in spring equation


%Inertia comparisson

resolution=.01;
x=[0:resolution:1]';
J_strict_net=zeros(length(x),1);
M_strict_net=zeros(length(x),1);
J_lin_net=Jlinfind(Ro2find(1/5))*ones(length(x),1);
M_lin_net=Mlinfind(Ro2find(1/5))*ones(length(x),1);

R_o_strict_squared = zeros(length(x),1);
J_strict_mequiv=zeros(length(x),1);
J_strict=zeros(length(x),1);
m_strict=zeros(length(x),1);


for i=1:length(x)
    J_strict(i) = Jfind(x(i));
    M_strict(i) = Mfind(x(i));
    R_o_strict_squared(i) = Ro2find(x(i));
    J_strict_net(i) = Jnetfind(J_strict(i),M_strict(i),R_o_strict_squared(i));
    M_strict_net(i) = Mnetfind(J_strict(i),M_strict(i),R_o_strict_squared(i));
    J_strict_mequiv(i)= Jstrictmequivfind(J_strict(i), R_o_strict_squared(i));
```

```
end

figure(17)
plot(x, J_strict_net)
hold on
plot(x, J_lin_net)
hold off
axis([0 5 0 2.2e-5])

figure(171)
plot(x, M_strict_net)
hold on
plot(x, M_lin_net,'-.')
plot(x, J_strict_mequiv,'--')
plot(x, M_strict,':')
hold off
axis([0 5 0 .5])
title('Comparison of simple and full model inertia terms')
legend('Full effective mass','Simple predicted mass','Full effective mass of coil','M
xlabel('Tip position (m)')
ylabel('Mass (kg)')
print masscomparefig -depsc

%Force Comparisson
resolution=.01;
x=[0:resolution:1]';
F_strict=zeros(length(x),1);
Ffind(1/2)
F_lin=Ffind(1)*ones(length(x),1);
%F_lin=Ffind(0)*ones(length(x),1);


R_o_strict_squared = Ro2find(0);

for i=1:length(x)
    F_strict(i) = Ffind(x(i));
end

figure(27)
plot(x, F_strict,'LineWidth',1.5)
hold on
plot(x, F_lin,'-.','LineWidth',1.5)
hold off
axis([0 5 0 825])
title('Comparison of simple and full model force terms')
```

```
legend('Force under full model','Force under simple model','location','east')
xlabel('Tip position (m)')
ylabel('Force (N)')
print forcecomparefig -depsc
%Unrolling simulation




done = 1

function [Jstrict] = Jfind(x)
%finds strict solution of coil inertia for a given position
    global rho t l D alpha E nu w gmma;
    Jstrict = rho*t*w*(l-x)*(D^2/4+(t*(l-x))/(2*pi));

function [Mstrict] = Mfind(x)
%finds mass of sliding portion as for given position
    global rho t l D alpha E nu w gmma;
    Mstrict = rho*t*w*x;

function [Ro2] = Ro2find(x)
%finds the outer radius of the coil for given position
    global D t l;
    Ro2 = D^2/4+(t*(l-x))/pi;

function [Jstrictnet] = Jnetfind(J,M,Ro2)
%finds the net inertia seen at the drive axle of the spool
    Jstrictnet = J+M*Ro2;

function [Jstrictmequiv] = Jstrictmequivfind(J,Ro2)
%finds the net inertia seen at the drive axle of the spool
    Jstrictmequiv = J/Ro2;


function [Mstrictnet] = Mnetfind(J,M,Ro2)
%finds the net mass seen anywhere along the formed tube
    Mstrictnet = J/Ro2+M;

function [Jlin] = Jlinfind(xbase2)
%finds the linear approximation of the total inertia
%for a given working radius
    global rho t l D alpha E nu w gmma;
    Jlin = rho*t*w*l*xbase2;
```

```
function [Mlin] = Mlinfind(xbase2)
%finds the linear approximation of the total inertia
%for a given working radius
    global rho t l D alpha E nu w gmma;
    Mlin = rho*t*w*l;

function [F] = Ffind(x)
%Finds the unrolling force as a function of x
    global rho t l D alpha E nu w gmma;
    Y=l-x;
    K=(E*gmma*pi*t^3)/((1-nu^2)*6*D);
    a=D^2;
    b=2*nu*D;
    f=D^2;
    c=4*t/pi;
    H=f+c*Y;
    F=K*(1+a/(H)+b/(H)^.5);

function [Vstrict] = Vfind(x)
%finds the stored energy in the coil as a function of x
    global rho t l D alpha E nu w gmma;
    Y=l-x;
    K=(E*gmma*pi*t^3)/((1-nu^2)*6*D);
    a=D^2;
    b=2*nu*D;
    f=D^2;
    c=4*t/pi;
    H=f+c*Y;
    Vstrict = K*(Y + a/c*log((H)/f) + 2*b/c*((H)^.5-f^.5));

function [Vlin] = Vlinfind(x,xbase)
%Finds the stored energy in the coil as a function of x
%for the approximation of constant bend radius equal to
%that found at the operating point of x=xbase
    global rho t l D alpha e nu w gmma;
    Y=l-x;
    K=(E*gmma*pi*t^3)/((1-nu^2)*6*D);
    a=D^2;
    b=2*nu*D;
    f=D^2;
    c=4*t/pi;
    H=f+c*Y;
    V=K*Y*(1+a/(H)+b/(H)^.5);
```

Bibliography

[1] alpha gear drives Inc. Rack and pinion system offers high linear accuracy, alpha gear drives, inc. http://news.thomasnet.com/fullstory/14401.

[2] A. H. Bohr. Extensible and retractable member. US Patent 3213573.

[3] Aerial Specialists Inc. Condor scissor lift. http://www.aerialspecialists.com/sitebuildercontent/Condor_Scissor_Lift.gif.

[4] Genie Inc. Genie runabout. http://www.genielift.com/runabout.asp.

[5] Ribbon Lift Inc. Ribbon lift actuators for lift applications - compact, portable and versatile. http://ribbonlift.com/.

[6] Serapid USA Inc. Serapid - theatre - vertical range - applications and advantages. http://serapid.com/gb/theatre/th_app_av_gb.html.

[7] Thomas W. Murphey and Sergio Pellegrino. A novel actuated composite tape spring for deployable structures. In *45th AIAA/ASME/ASCE/AHS/ASC Structures, Structural Dynamics and Materials Conference*, Palm Springs, CA, 19-22 April 2004. Hosted and published by AIAA. AIAA-2004-1528.

[8] S. Pellegrino and S. D. Guest, editors. *IUTAM-IASS Symposium on Deployable Structures: Theory and Applications*, Cambridge, UK, September 1998. IUTAM-IASS, Kluwer Academic Publishers, Dordrecht/Boston/London.

[9] F. P. J. Rimrott. Storable tubular extendable member. *Machine Design*, 37(28):156–165, December 9, 1965 1965.

[10] F. P. J. Rimrott and G. Fritzche. Fundamentals of stem mechanics. In Pellegrino and Guest [8], pages 321–323.

[11] K. A. Seffen and S. Pellegrino. Deployment dynamics of tape-springs. *Proceedings of the Royal Society of London A*, 455:1003–1048, 1999.

[12] V. V. Sidorenko. Deployment dynamics of flexible beams. In Pellegrino and Guest [8], pages 365–371.

[13] Northrop Grumman Space Technology. Ds-101-bistemactuator.pdf. http://www.st.northropgrumman.com/astro-aerospace/SiteFiles/docs/pdfs/DS-101-BiStemActuator.pdf.